MASTER COPY KEEP THIS COPY FOR REPRODUCTION PURPOSES

REPORT DOCUMENTATION PAGE

Form Approved
OMB No. 0704-0188

1. AGENCY USE ONLY (Leave blank)	2. REPORT DATE	3. REPORT TYPE AND DATES COVERED
	11/14/94	Final 7/91-9/94

4. TITLE AND SUBTITLE
Real-Time X-Ray Scattering Study of Processing of High Performance Thermoplastics

5. FUNDING NUMBERS
DAAL03-91-G-0132

6. AUTHOR(S)
Professor Peggy Cebe

7. PERFORMING ORGANIZATION NAME(S) AND ADDRESS(ES)
Prof. Peggy Cebe
Massachusetts Institute of Technology
77 Mass. Ave., Rm. 13-5082
Cambridge, MA 02139

8. PERFORMING ORGANIZATION REPORT NUMBER

9. SPONSORING/MONITORING AGENCY NAME(S) AND ADDRESS(ES)
U. S. Army Research Office
P. O. Box 12211
Research Triangle Park, NC 27709-2211

10. SPONSORING/MONITORING AGENCY REPORT NUMBER
ARO 28369.5-MS

11. SUPPLEMENTARY NOTES
The view, opinions and/or findings contained in this report are those of the author(s) and should not be construed as an official Department of the Army position, policy, or decision, unless so designated by other documentation.

12a. DISTRIBUTION/AVAILABILITY STATEMENT
Approved for public release; distribution unlimited.

12b. DISTRIBUTION CODE

13. ABSTRACT (Maximum 200 words)

The purpose of the research was to use real-time X-ray scattering: 1) to assist in development of a model for the shrinkage of thermoplasti polymers during processing, and 2) to study the kinetics of crystal structure development. The principl tasks involved real-time X-ray scattering experiments. The secondary tasks involved characterization studies of the materials. We are using real-time X-ray scattering to study the shrinkage of crystallizable thermoplastic polymers during heat treatment. Most processing models in use today do not use data collected in-situ. The matrix shrinkage is determined in real time, directly from x-ray scattering. The evolution of cell structure that develops during crystallization can be detected by small angle and wide angle real-time x-ray scattering.

14. SUBJECT TERMS
x-ray scattering, thermoplastics, crystal structure

15. NUMBER OF PAGES
25

16. PRICE CODE

17. SECURITY CLASSIFICATION OF REPORT	18. SECURITY CLASSIFICATION OF THIS PAGE	19. SECURITY CLASSIFICATION OF ABSTRACT	20. LIMITATION OF ABSTRACT
UNCLASSIFIED	UNCLASSIFIED	UNCLASSIFIED	UL

REAL-TIME X-RAY SCATTERING STUDY OF PROCESSING OF HIGH PERFORMANCE THERMOPLASTICS

FINAL REPORT

Professor Peggy Cebe

November 7, 1994

THE U.S. ARMY RESEARCH OFFICE

CONTRACT DAAL03-91-G-0132

Department of Materials Science and Engineering
Massachusetts Institute of Technology
Cambridge, MA 02139

TABLE OF CONTENTS

List of Figures

1. SUMMARY OF ACCOMPLISHMENTS (7/91-9/94)

1.1 Highlights of DAAL03-91-G-0132

1.1.1 Research Accomplishments (experimental method used)

1. Developed experimental methods to analyze thermal expansion coefficients of semicrystalline polymers *in-situ* during processing (real-time high temperature wide and small angle X-ray scattering, WAXS and SAXS, respectively)

2. Demonstrated use of electron density correlation function to measure crystallinity of polymers *in-situ* during processing (SAXS)

3. First determination of the coefficient of thermal expansion for PBT crystals and PBT amorphous phase (real-time high temperature WAXS and SAXS).

4. First development of a methodology for determining the thermal expansion coefficient of the *amorphous* phase in semicrystalline polymers (real-time high temperature WAXS and SAXS).

5. First demonstration that blends of PBT/PAr have interlamellar structure only for low PAr fractions (WAXS and SAXS).

6. First demonstration that PBT crystals exhibit melting point depression in blends with PAr, leading to negative Flory interaction parameter; first report of thermodynamic melting point of PBT/PAr blends (thermal analysis).

7. First observation of peak splitting of the ortho carbons in PBT crystals due to differences in local nuclear magnetic environment (solid state ^{13}C NMR).

1.1.2 Budget

Amount Spent as of 9/30/94	$239,475
Time Period of Expenditure	40 months
Total Budget	$239,475
Total Period of Grant	40 months*

* A no cost extension was granted for 5/94-9/94

11.3 Students Supported (months of support) and Present Status

Yao-Yi Cheng (7)	Ph. D., MIT, expected 2/95
Peter Pengtao Huo(10)	Ph. D., MIT, 2/93
Linda K. Molnar(11)	Ph. D., MIT, expected 2/96
Mark Homer(9)	S. B., MIT, 6/94
Paul Kang(9)	S. B., MIT, expected 6/96
Congpa You(6)	Employed at Microsoft

1.1.4 Publications and Presentations (Complete citations in 1.2)

Five major publications in refereed journals
Five publications in conference proceedings
Eight invited presentations
Ten contributed papers

1.1.5 Collaborations Established

Dr. Malcolm Capel is beam line manager of the X12B beam at the Brookhaven National Synchrotron Light Source and a faculty member of the *Brookhaven Biology Department*. Dr. Capel is co-author on research performed at NSLS and funded under this contract.

Dr. Heidi Schreuder-Gibson is a synthetic polymer chemist at the *U.S. Army Natick Research, Development and Engineering Center*. We are collaborating on a project in thermotropic liquid crystal-line polymers which have application potential in Soldier Protection. I am using real-time x-ray scattering to characterize phase transformations in LCPs synthesized by Dr. Schreuder-Gibson.

Dr. Mary Garbauskas is a scientist at the Corporate Research Center of the *General Electric Corporation*. Dr. Garbauskas became interested in the use of real-time x-ray scattering to study blends made by GE. She is supplying me with blend materials of PBT with polycarbonate.

Dr. Jerry Chung is a research scientist at the *Allied Signal Corporation*. Dr. Chung was my first Ph. D. student and is working in the area of blend synthesis and processing. He has provided many injection molded plaques of PET/PAr blends for SAXS studies.

Dr. Rose Ryntz is a scientist at the research center of *Ford Motor Company*. Dr. Ryntz is studying failure of paint to adhere to car bumpers made of semicrystalline blends. She is interested in our use of real-time x-ray scattering to monitor phase transformations during melt processing of blends. Dr. Ryntz has provided us with film samples of polypropylene.

Dr. Dave Shiraldi is a scientist at *Hoechst Celanese* whom I met at the Asilomar Polymer Physics Conference. Dr. Shiraldi has provided me with a series of polymers of carefully controlled structure in the polyester family.

1.2 Publications and Presentations Resulting from DAAL03-91-G-0132

1.2.1 Papers in Refereed Journals

1. Peter Pengtao Huo, Peggy Cebe, and Malcolm Capel. "Real-Time X-Ray Scattering Study of Thermal Expansion of Poly(butylene terephthalate)." *J. Polymer Science, Polymer Physics. Ed.*, 30, 1459-1468 (1992).

2. Peter Pengtao Huo, Peggy Cebe, and Malcolm Capel. "Dynamic Mechanical and X-ray Scattering Study of Poly(butylene terephthalate) /Polyarylate Blends." *Macromolecules*, 26, 4275-4282 (1993).

3. Peter Pengtao Huo and Peggy Cebe. "^{13}C Solid State NMR Study of PBT/PAr Blends." *Macromolecules*, 26, 5561 (1993).

4. Peter Pengtao Huo and Peggy Cebe. "Melting Point Depression in Poly(butylene terephthalate)/Polyarylate Blends." *Macromolecules*, 26, 3127-3130 (1993).

1.2.2 Papers in Conference Proceedings

1. Peter Pengtao Huo, Peggy Cebe and Malcolm Capel. "Real Time SAXS Studies of Poly(butylene terephthalate)/ Polyarylate Blends." American Chemical Society, *Polymer Preprints*, 33(2), 446-447 (1992).

2. Peter Pengtao Huo and Peggy Cebe. "Melting Point Depression in Poly(butylene terephthalate)/Polyarylate Blends." American Chemical Society, *Proceedings of the Division of Polymer Materials Science and Engineering*, 68, 302-303 (1993).

3. Peter Pengtao Huo, Peggy Cebe, and Malcolm Capel. "Characterization of Polymer Structure Using Real-Time X-ray Scattering." In *Non-destructive Characterization of Materials, VI*, Eds: R. E. Green, K. J. Kozaczek, and C. O. Ruud (Plenum Press, 1994) p. 749-756.

4. Peggy Cebe, Paul Kang, and Ingchie Kwan. "Drawing of Poly-(phenylene sulfide)." *Proceedings of 52nd Annual SPE-ANTEC,* Symposium on Advanced Polymer Composites, XL(II), 1491 (1994).

5. Peter Pengtao Huo, Peggy Cebe, and Malcolm Capel. "Small Angle X-ray Scattering of Polymer Blends." *Proceedings of the Materials Research Society,* Symposium on Crystallization and Related Phenomena in Amorphous Materials: Ceramics, Metals, Polymers, and Semiconductors, Eds: M. Libera, T. Haynes, P. Cebe, and J. Dickenson, 321, 555 (1994).

1.2.3 Invited Talks

1. October 1992, "Blends of Semicrystalline and Amorphous Polymers." Seminar, Case Western Reserve University, Cleveland, OH.

2. November 1992, "Blends of Semicrystalline and Amorphous Polymers." Seminar, Institute for Materials Science, University of Connecticut, Storrs, CT.

3. June 1993, "Characterization of Polymer Structure Using Real-Time X-ray Scattering," Sixth International Conference on Nondestructive Evaluation of Materials, Oahu, HI.

4. November 1993, "High Temperature X-ray Scattering Study of Crystalline Polymers," Dartmouth College, Hanover, NH.

5. January 1994, "High Temperature X-ray Scattering of Polymers and Blends." Seminar, Rensselear Polytechnic Institute, Troy, NY.

6. February 1994, "Real Time X-ray Scattering of Polymers and Blends," *Asilomar Conference* on Polymers, Monterey, CA.

7. April 1994, "High Temperature X-ray Scattering from Polymers," Seminar, University of Florida, Gainsville, FL.

8. August 1994, "Real Time X-ray Scattering of Polymers and Blends," Denver X-ray Conference, Denver, CO.

1.2.4 Contributed Talks and Posters

1. March 1992, "C-13 NMR of Blends of Poly(butylene terephthalate)/ Poly(arylate), PBT/PAr." American Physical Society Symposium of Division of High Polymer Physics, Indianapolis, IN.

2. April 1992, "^{13}C-Solid State NMR of Blends of poly(butylene terephthalate)/polyarylate, PBT/PAr." American Chemical Society Symposium on Molecular Dynamics, San Francisco, CA.

3. August 1992, "Real-Time SAXS Study of Poly(butylene terephthalate/ Polyarylate) Blends." American Chemical Society Symposium on Blends of Amorphous and Crystalline Polymers, Washington, D.C.

4. December 1992, "Structure of Poly(butylene terephthalate/ Polyarylate) Blends." Materials Research Society Symposium on Polymer Blends, Boston, MA.

5. December 1992, "Real-Time X-Ray Scattering Study of Morphology Development in Blends of Semicrystalline and Amorphous Polymers." Materials Research Society Symposium on Polymer Blends, Boston, MA.

6. March 1993, "Melting Point Depression in Poly(butylene terephthalate)/ Poly(arylate) Blends." American Physical Society Symposium on Morphology I, Seattle, WA.

7. March 1993, "Structure of Poly(butylene terephthalate)/ Poly(arylate) Blends." American Physical Society Symposium on Morphology II, Seattle, WA.

8. March 1993, "Melting Point Depression in Poly(butylene terephthalate)/ Poly(arylate) Blends." American Chemical Society Symposium on Thermal Analysis, Denver, CO.

9. December 1993, "Real-Time X-ray Scattering Studies of Polymer Blends." Materials Research Society Symposium on Crystallization and Related Phenomena, Boston, MA.

10. May 1994, "Spherulite Deformation in Poly(phenylene sulfide)." Society of Plastics Engineers, San Francisco, CA.

2.0 RESEARCH ACCOMPLISHMENTS

The purposes of the research were to use real-time X-ray scattering: 1.) to assist in development of a model for the shrinkage of thermoplastic polymers during processing, and 2.) to study the kinetics of crystal structure development. Two parallel lines of research were conducted. The principal tasks involved real-time X-ray scattering experiments. The secondary tasks involved characterization studies of the materials. Since beam time at the Brookhaven National Synchrotron Light Source (NSLS) is given in discrete blocks, our real-time X-ray studies were performed over a total of seven trips. Data from the sixth trip is analyzed and in the process of being written up. Data from the last trip (April 1994) have not been completely analyzed. Our collaboration with Dr. Malcolm Capel has proven to be extremely beneficial, and we have been very successful in getting beam time allocated through the NSLS General Users Program. Our last proposal, for beam time in 1992-1994, was rated very highly at 1.9 (1.0 is highest, 5.0 lowest) and we received 18 days of beam time. The materials selection and characterization studies are described in sections 2.1 and 2.2. The real-time x-ray scattering studies are described in sections 2.3 and 2.4.

2.1 Materials Selection and Preparation

We selected for our study a semicrystalline polyester that is used both as neat material, and as matrix for glass fiber reinforced composites. The polymer is poly(butylene terephthalate), PBT. This polymer can be blended with amorphous polyarylate, PAr, to improve mechanical properties and increase the glass transition temperature. In Figure 1, the chemical structures of these polymers are shown. The reasons for our choice of PBT were: 1. it has a melting point of 250°C [1,2] in the range accessible for studies at NSLS; 2. it has rapid crystallization kinetics[2-5]; 3. it is commercially available from U. S. suppliers (e.g., General Electric); 4. it is important for U. S. industry[6]; 5. it exhibits a solid-solid phase transformation under stress[7-10] making it a good subject for the next phase of our study. Finally, though its crystal structure had been reported previously [7-9,11-16], there were no real-time studies of structure development, and no reports of crystal or amorphous phase expansion coefficients.

In another study, we chose to focus on the real-time study of structure development in blends of semicrystalline with amorphous polymers. Here we chose the PBT/PAr system. This choice was advantageous because only a few reports existed about blend structure, though the blend pair is one of few which is miscible over the entire composition range in the melt [2,5,17-21].

PBT homopolymer was prepared from as-received powder (from Polysciences) by compression molding between ferrotype plates at 250°C for one minute, followed by quenching into ice water. Polyarylate was obtained from Amoco. Blends were prepared from phenol/TCE solutions according to the method of Kimura, et al.[17] in compositions 80/20, 60/40, 40/60, and 20/80. The precipitated blend powders were recovered, washed and dried under vacuum for several days. They were compression molded and quenched in a manner similar to the PBT homopolymer.

2.2 Characterization of Homopolymers and Blends

PBT and its blends with PAr were characterized using solid state ^{13}C nuclear magnetic resonance (NMR), differential scanning calorimetric (DSC) thermal analysis, dynamic mechanical analysis (DMA), and room temperature wide angle x-ray scattering (WAXS). Two manuscripts resulted from NMR and DSC characterization studies [2,21]. Several significant aspects of the polymer structure, heretofore unknown, were reported in these works. First, DSC analysis of melting points of PBT and blends showed for the first time that the blends had a melting point depression of the infinite crystal melting point, T_m^0. This is shown in Figure 2, which is a Hoffman-Weeks plot [22] of melting point, T_m vs. crystallization temperature, T_c. These are related according to the following expression:

$$T_m = T_m^0 (1-1/\gamma) + T_c/\gamma \qquad (1)$$

where γ is the thickening factor, relating the size of thickened lamellae to the size of the growing critical nucleus [23].

There is a systematic decrease in the infinite crystal melting point, as shown by the decrease in the intersection point of the data with the line $T_m=T_c$ as PAr fraction increases. The infinite crystal melting point is an important processing parameter, since it represents the temperature above which the molten polymer must be heated in order completely to erase effects of prior crystallization history. This characterization of the blends provides very important processing information that was not available before.

Second, the effect of addition of PAr on the crystallization kinetics of PBT was determined. PAr reduces the rate of crystallization of PBT at a given temperature [2,5,19]. This means that crystals of PBT form more slowly in the blends than in the homopolymer. Crystals formed in the blends were more perfect than those in homopolymer crystallized at the same temperature. For example, crystals in the 80/20 blend had narrower full width half maxima in WAXS and ^{13}C NMR [21]. Compared to other NMR studies of PBT [24-28], as a result of our more perfect crystals, we were able to observe for the first time

peak splitting of the ortho carbons of PBT crystals. We may conclude that the rate of phenyl ring flipping at room temperature must be very low in PBT crystals. Fast flipping rates would tend to average out local magnetic environment resulting in absence of peak splitting.

2.3 Real-Time X-ray Scattering Studies of Crystallization

X-ray scattering has been used extensively to study polymer structure (see [29-31] and references therein). We are using real-time X-ray scattering to study the shrinkage of crystallizable thermoplastic polymers during heat treatment [32]. When a polymer is processed from the melt, its volume changes as a result of: 1. development of more dense crystals, and 2. thermal contraction as the polymer cools. While thermal contraction results in small volume change relative to crystal formation, thermal expansion *mismatch* between matrix and composite fiber can be very large. Thus, we decided to treat both aspects of volume change in this research. Most processing models in use today do not use data collected in-situ. Instead, available processing models predict the polymer matrix behavior based on the degree of crystallinity determined from room temperature measurements after processing is completed, and from crystallization kinetics determined from thermal experiments[33-36]. One severe limitation of current processing models is that real polymer processing occurs under non-isothermal conditions. Attempts to model the non-isothermal processing are extensions of the Avrami analysis, which was developed to describe isothermal crystallization[37,38].

In our approach, the matrix shrinkage is determined in real time, directly from x-ray scattering. We use a controllable sample heating device (Mettler FP80 Hot Stage) so that the sample can be heated and cooled reproducibly for in-situ observation. To understand the mechanism of polymer crystal growth from the melt or from the rubbery amorphous state, information about the developing crystal structure should be collected nearly instantaneously during isothermal or non-isothermal crystallization. Experiments are performed by heating the semicrystalline polymer above its infinite crystal melting point to erase existing structure, then either a.) cooling down to a pre-set crystallization temperature, or b.) cooling at a fixed rate, or c.) quenching below T_g and then heating to crystallize from the rubbery state. The evolution of long period and unit cell structure that develop during crystallization can be detected by small angle and wide angle real-time x-ray scattering. In situ studies of this kind require very short exposures, and therefore very high intensity as well as high speed detection. The high intensity characteristic of the synchrotron x-ray beam allows the real-time measurement during melt crystallization even at large undercooling where the crystallization time is very short.

Our processing model is based on an equation for the change in volume of a known total mass of material, M, which cools and crystallizes. We assume that the volume, V, of material comprises the amorphous phase volume plus the crystal phase volume (two-phase assumption), and that no voids are formed. In that case, the material is densely filled with crystals and the amorphous phase. Using subscripts a for amorphous phase, and c for crystal phase, we write the volume at any time, t, and temperature, T, as:

$$V(T,t) = M/ \{\chi_c(T,t)\, \rho_c(T,t) + \chi_a(T,t)\, \rho_a(T,t)\} \qquad (2)$$

where χ_i, ρ_i are the volume fraction and density, respectively, of the i^{th} phase. It is convenient to write the denominator in a manner that shows the variables that are directly measured from SAXS and WAXS experiments. The volume at any time and temperature becomes:

$$V(T,t) = M/ \{(1-\chi_c(T,t))\, (\rho_a(T,t)-\rho_c(T,t)) + \rho_c(T,t)\} \qquad (3)$$

To obtain an experimental determination of V(T,t), we use WAXS to get ρ_c from the unit cell volume. With a two-phase assumption, we use SAXS to measure χ_c . For reviews of this approach, the reader is referred to Refs.[29-31,39,40]. $(\rho_a-\rho_c)$ would be obtained from the difference in the electron densities $(\rho_a{}^e-r_\chi{}^e)$ [40]. What is *unique* about our approach is that these parameters are obtained from x-ray scattering measurements made during processing.

Ideally, after the completion of processing, the volume of material given by equation (3) should be identical to the desired final volume, e.g., the volume of the mold in injection molding. Beside the actual direct measure of V(T,t) from parameters determined by x-ray scattering, we also want to develop *predictive* capability. In order to predict the final volume of material, we need to know the functional form of ρ_c, ρ_a, and χ_c with time and temperature. In this research, we have developed a method to determine both the crystal and amorphous phase thermal expansion coefficients (See Section 1.2.1, Ref. 1 and Section 1.2.2 Ref. 3). These coefficients relate the relative changes in density to changes in linear dimensions and are used to predict the change in volume.

In the next section we describe the use of WAXS to study the thermal expansion characteristics of the unit cell structure in PBT. Then we show how the volume fraction crystallinity and bulk thermal expansion can be determined from SAXS. Finally, we describe our new method to find the thermal expansion coefficient of the amorphous phase. These parameters of the polymer are required as input to the processing model.

Thermal Expansion of the Crystal Phase in PBT

We show WAXS intensity patterns at two temperatures for crystalline PBT in Figure 3. (Note, for this figure $\lambda = 0.91$Å.) The crystalline films display six well resolved peaks. The six reflections are indexed to (011), (010), (111), (011), (100) and (111). As the temperature increases from 35°C to 215°C all six peaks are found to have a significant shift to lower two theta angles. Using non-linear least squares fitting, we derive the six lattice parameters assuming the triclinic crystal structure proposed previously[7,8,11-15]. The lattice parameters at elevated temperature p(T) are related to their values, p_0 at 0°C, by:

$$p(T)=p_0 (1+ \alpha_l T) \tag{4}$$

where α_l is the linear thermal expansion coefficient, and T is the temperature in °C. We find the following relationships for the temperature dependence of the unit cell axes, a, b, c (Å), and angles, α, β, γ (degrees):

$$a = 4.80 (1+2.03 \times 10^{-4} T) \tag{5a}$$

$$b = 5.98 (1+1.22 \times 10^{-4} T) \tag{5b}$$

$$c = 11.55 (1+2.13 \times 10^{-4} T) \tag{5c}$$

$$\alpha = 100.26 (1+3.96 \times 10^{-5} T) \tag{5d}$$

$$\beta = 114.82 (1+8.13 \times 10^{-5} T) \tag{5e}$$

$$\gamma = 111.43 (1-3.92 \times 10^{-5} T) \tag{5f}$$

We observe increases in a, b, and c as a consequence of increasing temperature. The volume of the triclinic unit cell, V_c, can be calculated from the six lattice parameters. We find:

$$V_c = 258.0 (1 + 4.36 \times 10^{-4} T) \tag{6}$$

V_c increases as temperature increases, as shown in Figure 4. The unit cell volume at room temperature derived from eqn. (6) is in excellent agreement with previous reports [11-15].

This is the first report of the PBT crystal lattice thermal expansion behavior. The c-axis expansion for PBT is found to be about an order of magnitude larger than for poly(ethylene terephthalate), PET, its chemical relative. These results are consistent with elastic modulus measurements of the PBT and PET crystals [8]. Nakamae, et al. [8] report an unusually small

elastic modulus along the PBT chain, 13.5 GPa for PBT α-phase crystal, while for PET this value is 110 GPa, almost an order of magnitude larger. It has been observed that the main chain in PBT crystal lattice is more contracted than that of PET [7,8,11-15]. In the α form of PBT, the chain glycol segment has a GGTTGG conformation[7,8,15]. We therefore conclude that the difference in elastic modulus, and c-axis thermal expansion between PBT and PET is due to conformational differences.

Next, we describe our experiments using small angle X-ray scattering to study both the development of crystallinity and the thermal expansion of lamellar stacks in PBT.

Crystallinity and Bulk Thermal Expansion in PBT

In modeling the development of crystallinity in PBT, we assume that the polymer forms lamellar crystals, and that these will be arranged in stacks as shown in Figure 5. For our samples, the scattered intensity was isotropic, therefore we conclude that the lamellar stacks are also isotropically distributed throughout the sample volume. The one dimensional electron density correlation function, K(z), can be used to evaluate the X-ray scattering pattern taken while the polymer is crystallizing. K(z) is found from [39]:

$$K(z)=\int_0^\infty 4\pi\, I(s)s^2\cos(2\pi sz)ds \qquad (7)$$

where z is a dimension along the normal to the lamellar stack and s is the scattering vector ($s = 2\sin\theta/\lambda$). Here, I(s) is the corrected intensity after background and thermal density fluctuations have been subtracted. I(s) vs. s data are shown in Figure 6 for non-isothermal crystallization of quenched PBT during heating at 10°C/minute. Each intensity scan was recorded for 30 seconds, which means the intensity reflects an average over five degrees.

For the calculation of K(z), I(s) vs. s data are extrapolated to s=0 linearly and Porod's law [41], $I(s)\sim s^{-4}$, is used to extrapolate the intensity data to s=infinity. In Figure 7a, we show the general shape of K(z) vs. z for an ideal two-phase system with transition zones [39]. In Figure 7b experimental K(z) is shown for PBT at several temperatures. Long period, L, lamellar thickness, l_c, and crystallinity, χ_c, are obtained according to the method described by Strobl and Schneider [39]. The method is very accurate [39] for polymers with low or high degree of crystallinity, $\chi_c < 0.33$ or $\chi_c > 0.66$, a condition met by the polymers in our study. L is found from the position of the first maximum; l_c is found from the first intercept of K(z) with the baseline; χ_c is found from the first intercept of K(z) with the z-axis. From Figure 7b, we see that long period, lamellar thickness, and degree of crystallinity all increase as the temperature

increases. Knowing the time development of crystallinity during non-isothermal processing and the crystal lattice thermal expansion, we can predict the densification of the material due to crystal formation.

Using real-time SAXS combined with room temperature SAXS, we obtain the thermal expansion coefficient for the bulk material. Here, we compare long periods of two types of samples. One set is prepared by heating at 10°C/minute to a certain temperature where the long period is measured. The other set is prepared by heating at 10°C/minute to a certain temperature, then quickly cooling to room temperature. The difference in the long period between these two types of samples is due to the difference in the measurement temperature and not to differences of structure. We derive the average thermal expansion coefficient for the bulk material, α_{ave}, which is assumed to be isotropic, from:

$$L(T) = L(0)\,(1+ \alpha_{ave} \cdot T) \tag{8a}$$

$$L(T_0) = L(0)\,(1+ \alpha_{ave} \cdot T_0) \tag{8b}$$

where L(0) is the long period at T=0°C and T_0 is room temperature. Due to the small value of α_{ave} ($\alpha_{ave} \cdot T_0 << 1$) equation (8a) divided by (8b) evolves to the following:

$$L(T) = L(T_0)\,(1+ \alpha_{ave} \cdot (T-T_0)\,) \tag{9}$$

From the slope of a plot of $[L(T)/L(T_0)]-1$ vs. $T-T_0$ shown in Figure 8, we obtain the value of the bulk thermal expansion of PBT, $\alpha_{ave} = 5.0 \times 10^{-4} °C^{-1}$, which agrees very well with previous work [42].

Amorphous Phase Thermal Expansion in PBT

For the first time, we can calculate the thermal expansion coefficient for the amorphous phase by combining information from the crystal lattice thermal expansion with knowledge of the expansion of a lamellar stack. This parameter is very important because the densification of the melt depends upon the density changes in both the crystals and the amorphous phases. The amorphous phase expansion coefficient can not be directly measured by thermo-mechanical techniques, because these semicrystalline polymers generally crystallize immediately above T_g.

Our calculation gives an average expansion coefficient for the entire amorphous phase. The thermal expansion for the long period, L, can be viewed as the contribution from the crystal and amorphous layers, of thickness l_c and l_a, respectively. L and l_c are obtained directly from the one

dimensional electron density correlation function analysis[39], and $L=l_c+l_a$. Using the lamellar model of Figure 5, we write:

$$l_a(T) = L(T) - l_c(T) \tag{10a}$$

$$l_a(T_0) = L(T_0) - l_c(T_0) \tag{10b}$$

At elevated temperature, the l_c and l_a can be written in terms of their room temperature values as:

$$l_c(T) = l_c(T_0)\,(\,1+\alpha_c\cdot(T-T_0)\,) \tag{11a}$$

$$l_a(T) = l_a(T_0)\,(\,1+\alpha_a\cdot(T-T_0)\,) \tag{11b}$$

where α_c and α_a are the thermal expansion coefficients for the crystal phase and the amorphous phase in the direction along the normal to the lamellar stack.

We use equation (10a) to evaluate $l_c(T)$. Here, we assume that the thermal expansion coefficient of the crystal phase is not a function of temperature. A reasonable approximation for α_c is to assume it is close to the c-axis crystal lattice thermal expansion coefficient, $2.12\times10^{-4}\ C^{-1}$. From a plot of $[L_a(T)/L_a(T_0)]-1$ vs. $T-T_0$ shown in Figure 8, we find the thermal expansion coefficient for the amorphous phase to be $\alpha_a = 6.0\times10^{-4}°C^{-1}$. This is close to the bulk expansion coefficient [81,82], an expected result given the small degree of crystallinity in this polymer.

2.4 X-ray Scattering Studies of Blends

In this portion of the research, we used WAXS and SAXS to study the structure of blends. We are particularly interested in one type of melt-miscible polymer blend, where one polymer is amorphous and the other is crystallizable. Several of the most important blends available commercially are of this type. We chose for our study, blends of PBT/PAr which have been shown to be miscible at all compositions in the melt or in the amorphous state [2,17-20]. There exists a phase separation upon the crystalliz-ation of PBT, resulting in a crystal/amorphous lamellar structure [5,18,19].

We performed WAXS measurements for cold and melt crystallized blends in order to study the coherence length as a function of blend composition. This allows us to estimate the crystal sizes in the crystallo-graphic directions. Peak width has been shown to relate to the coherence length, t, by the Scherrer equation [30]:

$$t = K\lambda / \beta_{hkl} \cos\theta_{hkl} \quad (12)$$

where λ is the X-ray wavelength, β_{hkl} is the half width of peaks of Miller indices (hkl), θ_{hkl} is the scattering angle, and K is equal to 0.9 [30]. For PBT crystals, we assume that the c-axis is nearly perpendicular to the lamellar crystal fold surfaces and the coherence length determined from the (001) reflection may relate to the actual lamellar thickness. (The disposition of the c-axis relative to the lamellar surfaces is still unknown for this polymer.) Using equation (12) the lamellar thickness can be estimated from the (001) line broadening. The estimated lamellar thicknesses for PBT and PBT/PAr blends are listed in Table 1.

Room temperature static SAXS has been done on both the cold crystallized (T_c=180°C) and melt crystallized (T_c=200°C) PBT/PAr blends. We obtain the long period from the Lorentz corrected intensity maximum. The Lorentz corrected intensity vs. s data for the melt crystallized blend samples are shown in Figure 9. The long period L obtained from the intensity maximum as a function of blend composition is shown in Figure 10 for melt crystallized samples. The long period is nearly independent of the blend composition. For PBT homopolymer melt crystallized at 200°C, the long period is 138Å, while all melt crystallized blends have long periods ranging from 160Å to 180Å. The cold crystallized homopolymer and blends have long periods about 30Å shorter compared with their melt crystallized counterparts. The long period of cold crystallized PBT homopolymer is 100Å, while the long period of cold crystallized blends clusters in the range 120-150Å.

Table 1. Coherence Length in the a*, b*, and c* Directions for PBT/PAr Blends Melt Crystallized at 200°C

Blend	a*	b*	c*
100/0	100	160	50
80/20	120	180	50
60/40	150	200	50
40/60	200	190	50

The long period L is compared with the ratio of lamellar thickness (from Table 1) and total volume crystallinity, $v_{c,t}$. If $L=l_c/v_{c,t}$, we may conclude that the PAr location is interlamellar, while if $L<l_c/v_{c,t}$, the PAr location is interfibrillar or interspherulitic. Here the total volume fraction of crystallinity is obtained by the following:

$$\frac{1}{v_{c,t}} = 1 + \left(\frac{1-w_{c,p}}{w_{c,p}}\right)\left(\frac{\rho_1}{\rho_2}\right) + \left(\frac{x}{1-x}\right)\left(\frac{\rho_1}{\rho_3}\right)\frac{1}{w_{c,p}} \qquad (13)$$

where ρ_1, ρ_2, ρ_3 are the densities of PBT crystal (1.40 g/cm^3), amorphous PBT (1.28 g/cm^3) and PAr (1.21 g/cm^3) [17], respectively. x is the mass fraction of PAr in the blends, and $w_{c,t}$, $w_{c,p}$ are the total and partial mass fraction of crystallinity, which are related by:

$$w_{c,t} = w_{c,p}\,(1-x). \qquad (14)$$

Here, the direct implication is that whether or not each sample has interlamellar structure for the PAr is decided only by its own long period, lamellar thickness, and mass fraction of crystallinity. Knowing $v_{c,t}$ and lamellar thickness, l_c, from WAXS, and assuming an interlamellar structure, we also show the *calculated* L in Figure 10 (solid circles), as a comparison to the experimentally observed long period (open circles). As PAr composition increases the difference between observed L and calculated L increases. These results show that as PAr composition increases, an interlamellar placement becomes less probable. For blends with PAr>0.40 interfibrillar or inter-spherulitic placement of PAr is favored. One important conclusion of this work is that the placement of PAr can not be deduced from the trend of long period with composition. Instead it is necessary to compare the measured long period to the calculated long period for each blend independently.

From a commercial standpoint, it is extremely important for polymer processors to be able to predict blend structure after thermal treatment. In fact, several of our industrial collaborations (with General Electric, Allied Signal, Ford Motor) involve studies of blend structure. Polymer blends will occupy an increasing market share as manufacturers attempt to obtain property balance through compositional variation. Our blend research has generated the most enthusiastic response from U. S. industry.

3. BIBLIOGRAPHY

1. Valero, M.; Iruin, J. J.; Espinoza, E.; Fernandez-Berridi, M. J. *Polymer Comm.*, **1990**, *31(4)*, 127.
2. Huo, P. P.; Cebe, P. *Macromolecules*, **1993**, *26*, 3127.
3. Cheng, S. Z. D.; Pan, R.; Wunderlich, B. *Makromol. Chem.*, **1988**, *189*, 2443.
4. Yeh, J. T.; Runt, J. *J. Polym. Sci., Polym. Phys. Ed.*, **1989**, *27*, 1543.
5. Huo, P.; Cebe, P. Capel, M. *Macromolecules*, **1993**, *26*, 4275.
6. Porter, R. S.; Wang, L. H. *Polymer*, **1992**, *33*, 2019.
7. Roebuck, J.; Jakeways, R.; Ward, I. M. *Polymer*, **1992**, *33(2)*, 227.
8. Nakamae, K.; Kameyama, M.; Yoshikawa, M.; Matsumoto, T. *J. Polym. Sci., Polym. Phys. Ed.*, **1982**, *20*, 319 .
9. Smith, J.; Kibler, C.; Sublett, B. J. *J. Polym. Sci., Part A*, **1966**, *4*, 1851.
10. Nitzsche, S.; Wang, Y. K.; Hsu, S. L. *Macromol.*, **1992**, *25*, 2397.
11. M. Yokouchi, Y. Sakakibara, Y. Chatani, H. Tadokoro, T. Tanaka, and K. Yoda. *Macromol.*, **1976**, *9(2)*, 266.
12. Mencik, Z. *J. Polym. Sci., Polym. Phys. Ed.*, **1975**, *13*, 2173.
13. Stambaugh, B.; Koenig, J. L.; Lando, J. B. *J. Polym. Sci., Polym. Phys. Ed.*, **1979**,*17*, 1053.
14. Hall, I. H.; Pass, M. G. *Polymer*, **1976**, *17*, 807.
15. Desborough, I. J.; Hall, I. H. *Polymer*, **1977**, *18*, 825.
16. Peszkin, P.; Schultz, J. M. *J. Polym. Sci., Polym. Phys. Ed.*, **1986**, *24*, 2617.
17. Kimura, M.; Porter, R. S.; Salee, G. *J. Polym. Sci.: Polym. Phys. Ed.*, **1983**, *21*, 367.
18. Runt, J. P.; Zhang, X.; Miley, D. M.; Gallagher, K. P.; Zhang, A. *Macromolecules*, **1992**, *25*, 3902.
19. Runt, J. P.; Miley, D. M.; Zhang, X.; Gallagher, K. P.; McFeaters, K.; Fishburn,J. *Macromolecules*, **1992**, *25*, 1929.
20. Runt, J.; Gallagher, K. P. *Polym. Comm.*, **1991**, *32*, 181.
21. Huo, P.; Cebe, P. *Macromolecules*, **1993**, *26*, 5561.
22. Hoffman, J. D.; Weeks, J. J. *J. Res. Natl. Bur. Stand.* **1962**, *66*, 13.
23. Hoffman, J. D.; Davis, G. T.; Lauritzen, J. I. In "Treatise on Solid State Chemistry", Hanay, N. B., Ed.; Plenum Press: New York, **1975**, Vol. 3.
24. Jelinski, L. W.; Dumais, J. J.; Engel, A. K. *Macromolecules*, **1983**, *16*, 403.
25. Perry, B. C.; Koenig, J. L.; Lando, J. B. *Macromolecules*, **1987**, *20*, 422.

26. Garbow, J. R.; Schaefer, J. *Macromolecules*, **1987**, *20*, 819.
27. Gomez, M. A.; Cozine, M. H.; Tonelli, A. E. *Macromolecules*, **1988**, *21*, 388.
28. Cholli, A. L.; Dumais, J. J.; Engel, A. K.; Jelinski, L. W. *Macromolecules*, **1984**, *17*, 2399.
29. Alexander, L. E. *"X-ray Diffraction Methods in Polymer Science"* Wiley Interscience, John Wiley & Sons: New York, **1969**.
30. Kakudo, M.; Kasai, N. *"X-ray Diffraction by Polymers"*, Kodansha Ltd.: Tokyo, **1972**.
31. Balta-Calleja, F. J.; Vonk, C. G. "X-ray Scattering of Synthetic Polymers", Elsevier Sci. Pub.: Amsterdam, **1989**.
32. Huo, P.; Cebe, P.; Capel, M. *J. Polym. Sci., Polym. Phys. Ed.*, **1992**, *30*, 1459.
33. Seferis, J. *Polym. Comp.*, **1986**, *7(3)*, 158.
34. Seferis, J.; Ahlstrom, C.; Dillman, S. *SPE Antec, Tech. Papers*, **1987**, *21(11)*, 1467.
35. Velisaris, C.; Seferis, J. *Polym. Eng. Sci.*, **1986**, *26(22)*, 1574.
36. Springer, G. S. *"Manufacturing Thermoplastic Matix Composites"*, Tech. Info. Service Report #AD-A199724, July **1988**.
37. Avrami, M. *J. Chem. Phys.*, **1939**, *7*, 1103.
38. Avrami, M. *J. Chem. Phys.*, **1940**, *8*, 212.
39. Strobl, G. R.; Schneider, M. *J. Polym. Sci., Polym. Phys. Ed.*, **1980**, *18*, 1343.
40. Glatter, O.; Kratky, O. *Small Angle X-ray Scattering*, Academic Press Inc.: New York, **1982**.
41. Porod, G. *Kolloid Z.*, **1951**, *83*, 124.

Figure 1

CHEMICAL STRUCTURES

Poly(butylene terephthalate)

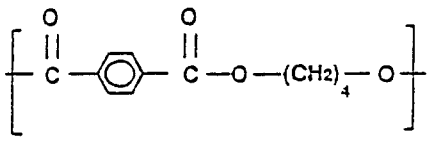

Polyarylate

50:50

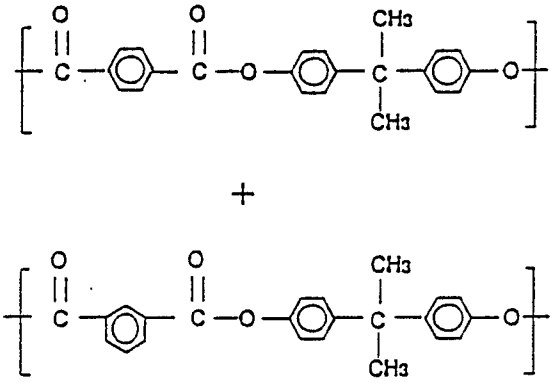

Figure 2

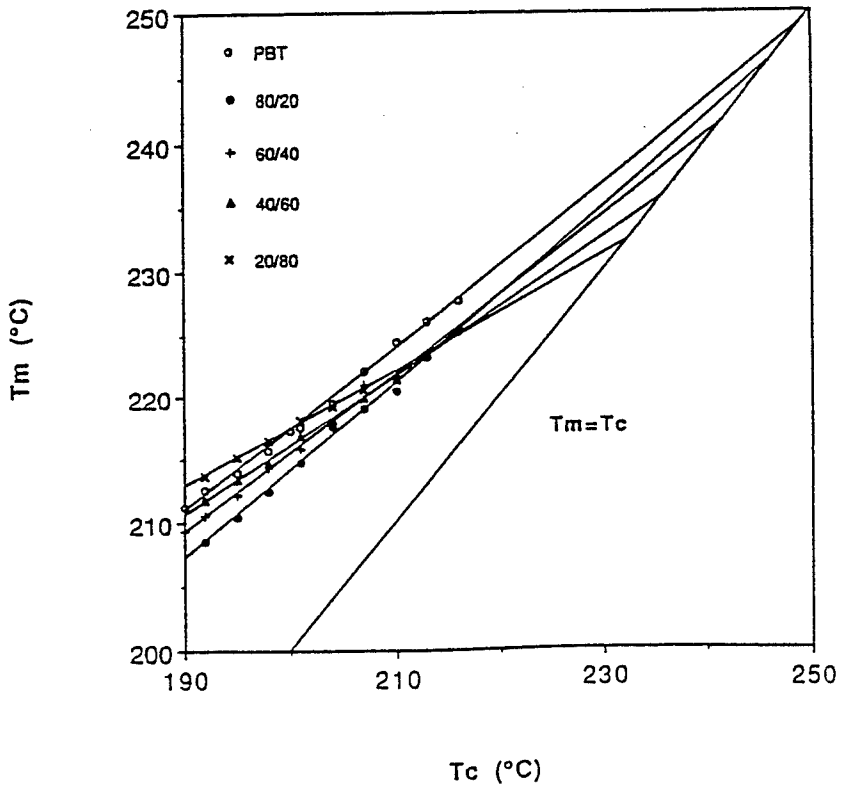

Figure 3

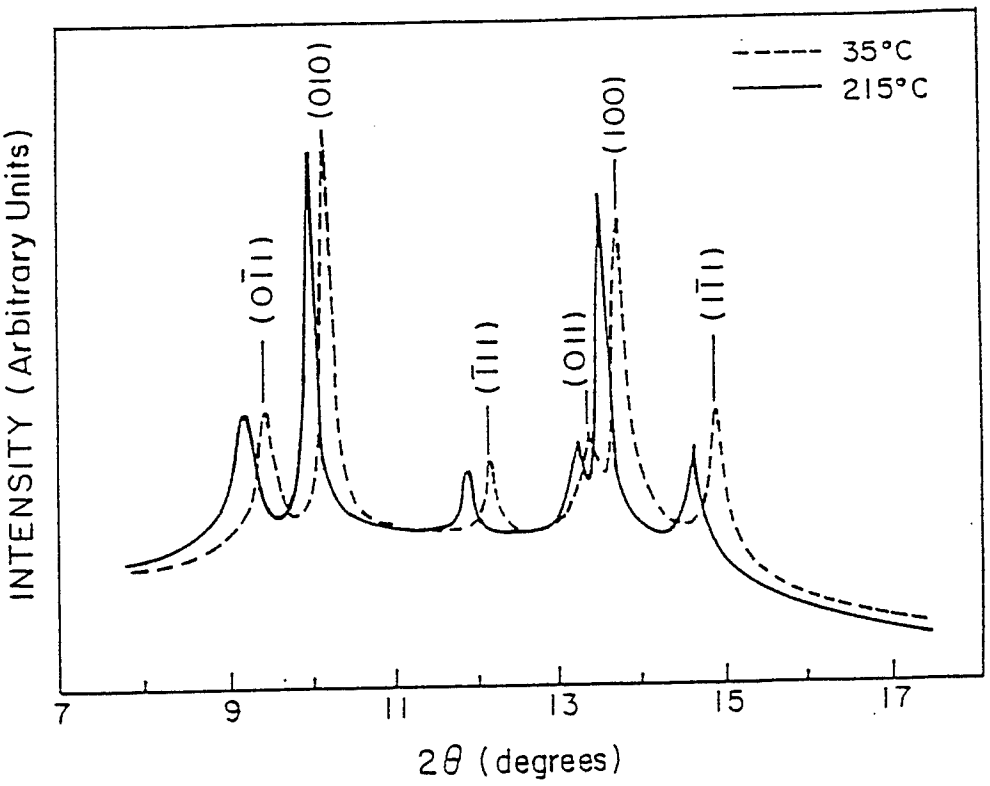

Figure 4

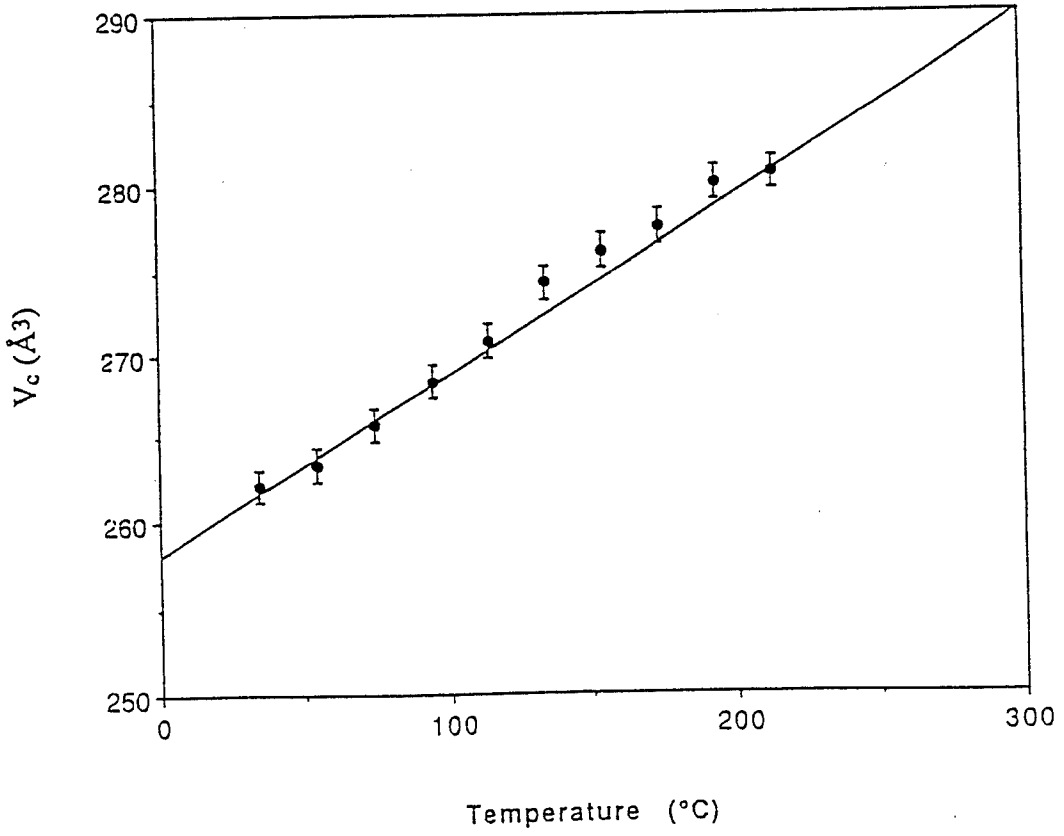

Figure 5

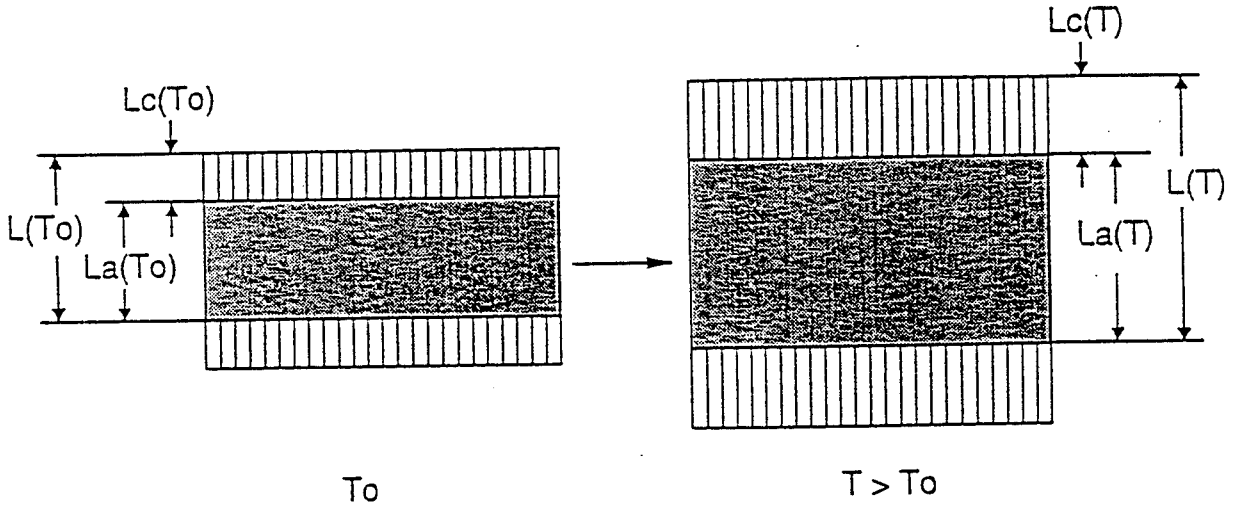

Figure 6

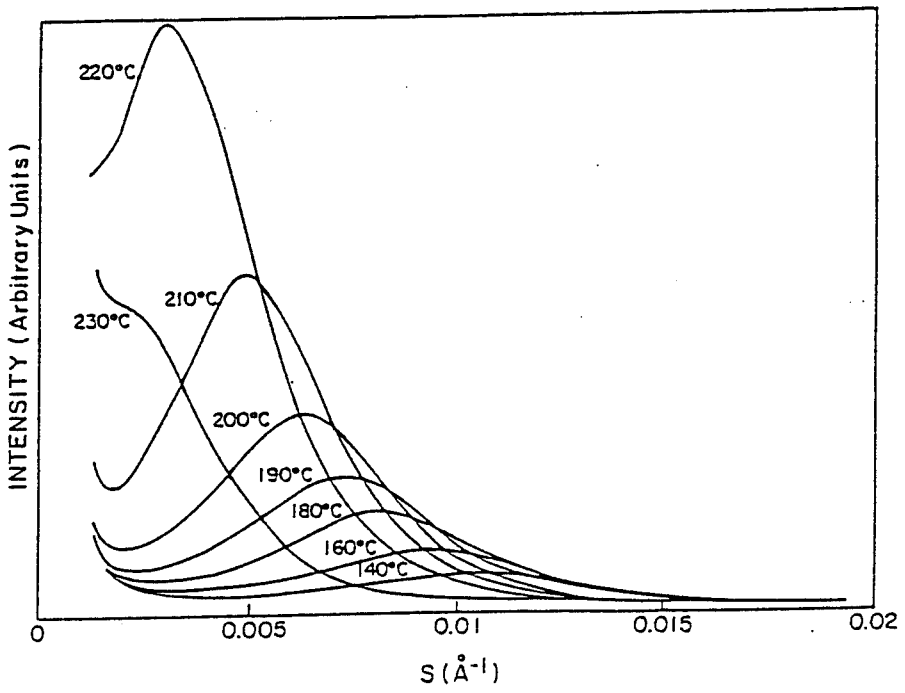

Figure 7a

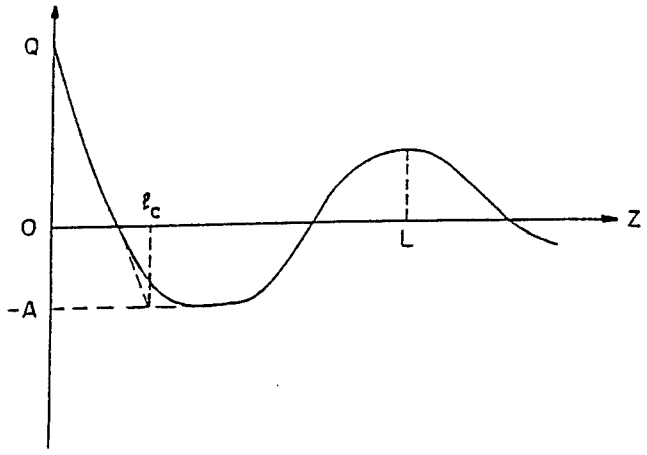

Figure 7b

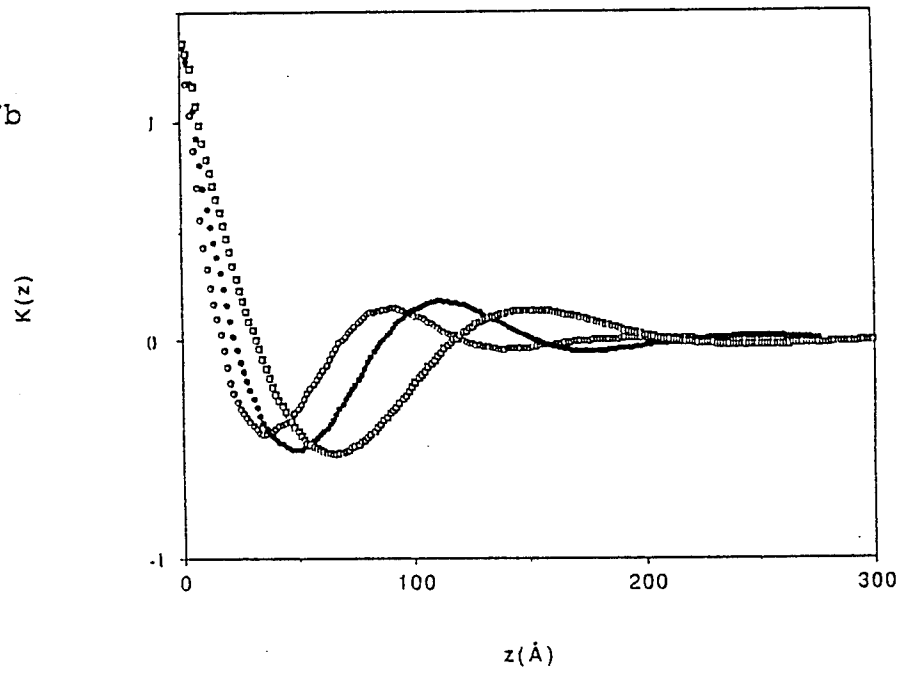

Figure 8

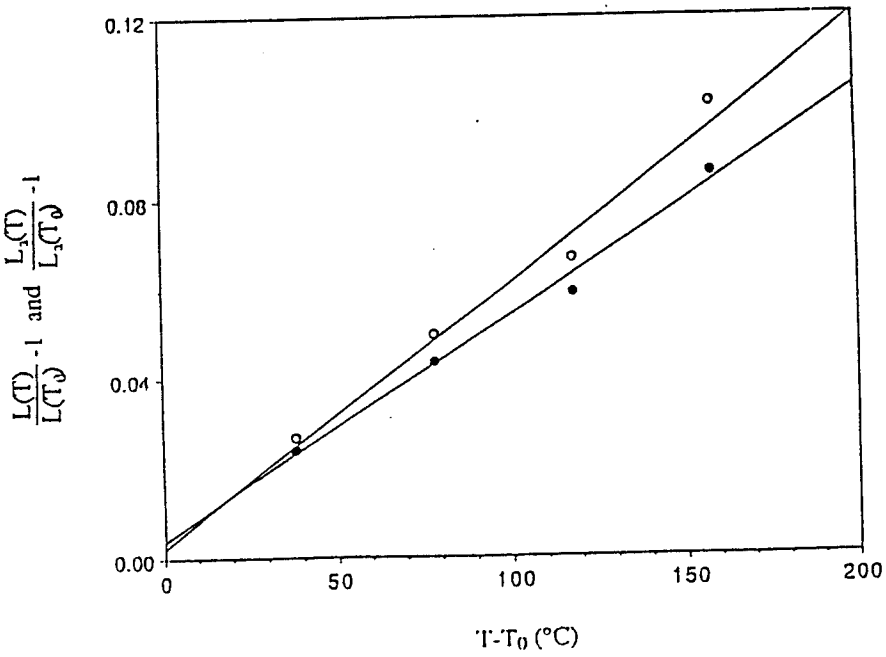

Figure 9

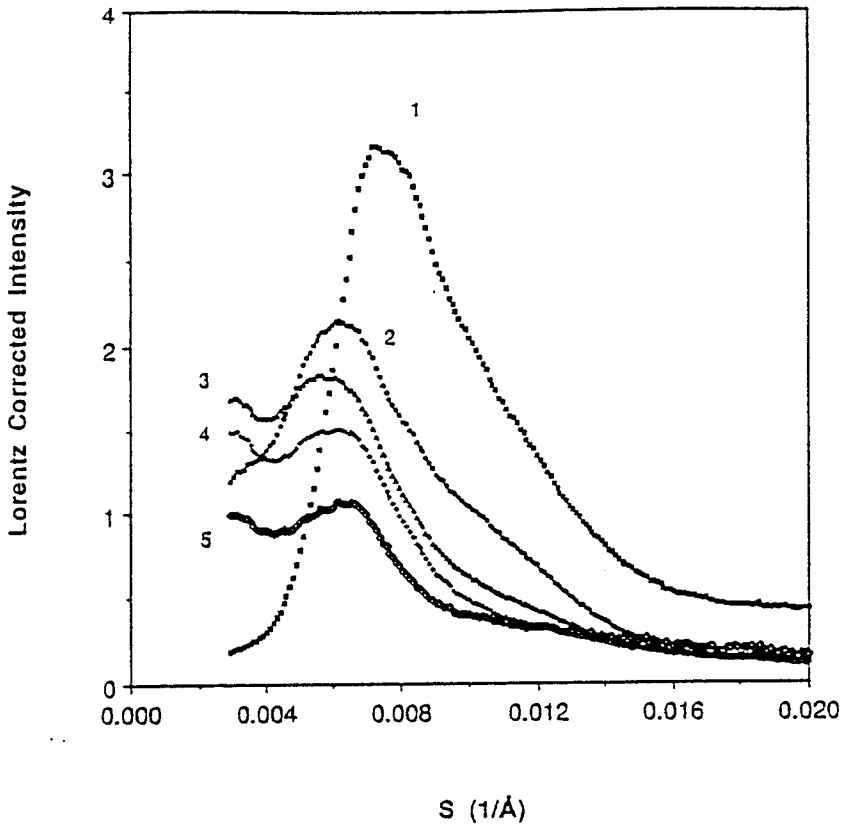

Figure 10